

Experimental section

Reagents and apparatus

Chemicals were purchased from J&K, Sigma-Aldrich, and TCI and used without further purification. Penicillin-streptomycin solution, trypsin-EDTA (0.5% trypsin and 5.3 mM EDTA tetrasodium), phosphate buffered saline (PBS, 1×), dulbecco's modified eagle medium (DMEM), and RPMI 1640 Medium (1640) were purchased from TransGen Biotech Co., Ltd. The ultracentrifuge, Optima-XPN-100, was bought from Beckman Coulter Corporation (U.S.). The scanning electron microscope (SEM) experiment was carried out using a Regulus 8100 (HITACH). From Abcam, we obtained goat anti-rabbit and goat anti-mouse IgG antibodies, CD9, TSG101, and Calnexin antibodies. Beyotime Biotechnology provided the Cell Counting Kit-8. A Shimadzu UV-2600 spectrometer was used to record UV-vis absorption spectra. The Hitachi F-4700 fluorescence spectrometer recorded photoluminescence (PL) spectra. The size and concentration of nanoparticles were determined using a Panalytical NanoSight NS300 (Malvern) and analyzed using Nanoparticle Tracking Analysis (NTA) software. The size distributions of nanoparticles were measured by dynamic light scattering (DLS) using a Malvern Zetasizer Nano ZS 3000. The Animal Care and Use Committee of Southern University of Science and Technology approved all animal experiments (SUSTC-2018-115).

Construction of AIE photosensitizer dataset

The scientific literature has extensively documented thousands of photosensitizers. We employed two specific criteria to screen the molecules during the data collection process. We prioritized AIEgen photosensitizers, a class of fluorophores that has demonstrated broad applicability in PDT. Then, we assessed whether the ROS quantum yield of each photosensitizer could be comparable to that of Rose Bengal, a highly efficient photosensitizer known to possess a 75% singlet oxygen quantum yield in water. This comparative analysis with Rose Bengal allowed us to judiciously limit the number of molecules in our dataset, mitigating the risk of an unbalanced and biased sample.

Screening molecular descriptors

Initially, we employed molecular descriptors to characterize molecules, encompassing two categories: quantitative descriptors and qualitative descriptors. Subsequently, the molecular descriptors undergo further screening, involving the removal of low variance and highly correlated features, resulting in the selection of 158 descriptors from an initial pool of 783.

Synthesis of photosensitizer

Chemicals 1-4 (1 mmol) and 1,4-dimethylquinolinium iodide (1.2 mmol) were dissolved in 10 mL of ethanol with a few drops of piperidine. The mixture was then refluxed under a nitrogen atmosphere for 24 h. After cooling to room temperature, the solution was concentrated under vacuum and purified using silica-gel chromatography with dichloromethane/ethanol as the eluent. The yield obtained was about 75%. The ¹H

and ^{13}C NMR spectra were recorded using Bruker AV400 instruments with DMSO as the solvents. HRMS data was collected using Q-Exactive with Dionex Ultimate 3000.

TP: 4-(4-(diphenylamino)styryl)-1-methylquinolin-1-ium iodide

MTP: 4-(4-(bis(4-methoxyphenyl)amino)styryl)-1-methylquinolin-1-ium iodide

TPP: 4-(2-(5-(4-(diphenylamino)phenyl)thiophen-2-yl)vinyl)-1-methylquinolin-1-ium iodide

MTPP: 4-(2-(5-(4-(bis(4-methoxyphenyl)amino)phenyl)thiophen-2-yl)vinyl)-1-methylquinolin-1-ium iodide

Detecting singlet oxygen production by ABDA

To evaluate the ability of singlet oxygen generation, we used 9,10-anthracenediylbis(methylene) malonic acid (ABDA) as an indicator. We mixed 20 μL of ABDA (10 μM) with 10 μM of RB, TP, MTP, TPP, and MTPP in 1.96 mL of deionized water as the reaction solution. The corresponding reaction solution was illuminated with white light (20 mW/cm^2) for 5 minutes. The absorption spectrum of ABDA was measured every 30 seconds, to plot the relative absorption intensity at 379 nm as a function of irradiation time. Additionally, under the same experimental conditions, we tested the change curve by adding only ABDA or the test sample as controls.

To compare the singlet oxygen production ability of Exosome, TPP, and ExoTPP after sonication, 10 μM ABDA was mixed with 5 μM ExoTPP or 4T1 exosome samples in PBS for measurement. Under white light irradiation of 20 mW/cm^2 for 5 minutes, the absorption spectrum of ABDA at 379 nm was measured every 30 seconds, to plot the relative absorption intensity as a function of time. Concurrently, the change curve for testing only ABDA is added as a control.

Cell culture

The Chinese Academy of Medical Sciences' Xiehe Cell Bank supplied the cells for purchase. The HeLa human cervical cancer cells were cultured in DMEM high glucose medium (Biological Industries, BI), and the 4T1 mouse breast cancer cells were cultured in RPMI 1640 medium (Biological Industries, BI), supplemented with 100 U/mL penicillin, 100 $\mu\text{g}/\text{mL}$ streptomycin and 10% heat-inactivated FBS, at 37 $^\circ\text{C}$ and 5% CO_2 .

Exosomes preparation

In 100 mm \times 20 mm dishes, 4T1 and HeLa cells were cultured for 48 h, reaching 70-80% confluency (3×10^7 cells). After that, the cell culture media were collected and stored at -80 $^\circ\text{C}$. Exosomes were extracted using sequential centrifugal procedures at 4 $^\circ\text{C}$. First, the collected culture media were centrifuged at 220 \times g for 10 min, followed by 2000 \times g for 20 min. The supernatant was collected and then centrifuged at 15,000 \times g. After that, the supernatant was filtered through a 0.2 μm filter (Acrodisc, America), followed by ultracentrifugation at 120,000 \times g for 70 min to pellet exosomes and finally resuspended in PBS.

Due to the subsequent ultrasound treatment involving exosomes, we performed the same ultrasound procedure on a portion of exosomes: pulsing a tip sonicator (Vibra-Cell VCX-500) with repeated on-off cycles at 10-second intervals for a total of three cycles, followed by incubation at 37 °C for 1 hour. We then used NTA for quantitative comparison.

Cellular uptake of autologous exosomes

Confocal microscopy was used to evaluate the cellular uptake of autologous exosomes. 4T1 cells-derived exosomes were labeled with Dio (green, Yeasen, China), a lipophilic fluorescent dye, in accordance with the manufacturer's instructions with a modification to observe the efficiency of cellular uptake. 4T1 and HeLa cells were cultured in confocal chambers and then co-cultured with Dio-labeled 4T1 cells-derived exosomes for 1 h, 4 h, 8 h, 12 h, and 24 h. The cells in the confocal chambers were fixed with 4% paraformaldehyde (PFA), washed with 1× PBS buffer (pH = 7.2-7.4) to remove the free exosomes, and then stained with DAPI (Beyotime, China). Confocal microscopy and ZEN software (Zeiss, Germany) were used to analyze the cellular internalization of Dio-labeled 4T1 exosomes in 4T1 cells and HeLa cells.

ExoTPP preparation and load efficiency measurement

The TPP-loaded exosomes (ExoTPP) were prepared using ultrasonic methods. Initially, TPP was dissolved in DMSO and subsequently mixed with exosomes in PBS at a ratio of 0.01 mmol TPP to 1×10^{12} exosome particles. To prevent cytotoxicity, the concentration of DMSO in PBS was kept below 1%. ExoTPP was generated by pulsing a tip sonicator (Vibra-Cell VCX-500) with repeated on-off cycles at 10-second intervals for a total of three cycles. The solution was then incubated at 37 °C for 1 hour.

We dissolved TPP and ExoTPP at the same concentration of 4 μM in 5 mL of PBS and centrifuged at $120,000 \times g$ for 70 minutes using a 5 mL centrifuge tube to precipitate exosomes while keeping TPP in solution. However, due to TPP's insolubility in water, both TPP-only and ExoTPP tubes showed significant precipitation, indicating that this speed cannot separate TPP. We then centrifuged at $15,000 \times g$ for 30 minutes, at which exosomes do not precipitate but TPP does. The supernatant of the ExoTPP tube retained the clear color of TPP, while the TPP-only tube supernatant appeared transparent. We measured the absorption in the supernatant using UV-Vis spectroscopy and compared it to the initial TPP concentration in ExoTPP preparation to determine loading efficiency.

Characterization of exosomes and ExoTPP

To investigate the morphology, particle size, and the presence of exosomal biomarkers, we employed dynamic light scattering (DLS) and nanoparticle tracking analysis (NTA) to measure the size distributions and concentrations of both exosomes and ExoTPP. Scanning electron microscopy (SEM) was also used to visualize the nanoparticles. Western blot analysis was performed to detect exosome-specific markers. The samples were incubated overnight with primary antibodies against CD9, TSG101, and Calnexin (1:1000, Abcam, UK). Subsequently, horseradish peroxidase-conjugated secondary

antibody was incubated with the samples for 2 h at room temperature. The ChampChemi 610 Plus (Beijing, China) visualized the protein signals.

Cytotoxicity study

Using a cytotoxicity study, we first studied the optimal concentration of TPP acting on tumor cells and then compared the phototoxicity of Exosomes, ExoTPP, and TPP under constant TPP concentration. To investigate the optimal concentration of TPP acting on 4T1 cells, a solution of 1mg/mL TPP dissolved in DMSO was prepared. The stock solution was diluted with a culture medium to avoid the concentration of DMSO exceeding 1%, which can affect cell activity. The present study utilized the Cell Counting Kit-8 (CCK-8) assay to evaluate the metabolic viability of 4T1 cells. The cells were seeded at a density of 5×10^3 cells per well in two 96-well plates. Following 24 h of incubation, the cells were treated with TPP solutions at concentrations of 1, 2, 4, 8, and 16 μ M and subsequently incubated for an additional 8 h in a dark environment, achieved by wrapping the plates with tin foil. One of the plates was then exposed to 10 mW/cm² of white light for 3 minutes before being wrapped again with tin foil. After another 24 h, CCK-8 solution was added to each well. The absorbance was measured at 450 nm using a microplate reader after 2 h (n = 6 in each loading concentration). Cell viability was expressed as the absorbance ratio of the TPP-treated cells to those incubated with culture medium only.

Afterward, based on the optimal TPP concentration obtained in the previous step, Exosomes, ExoTPP, and TPP were configured, and their phototoxicity was compared using the same experimental method.

***In vivo* anti-tumor effect**

To establish the 4T1 tumor-bearing mouse model, each female BALB/c mouse was subcutaneously inoculated with 1×10^6 4T1 cells in the right flank. 7 days later, the mice (30 in total) were randomly divided into six groups (5 in each group), followed by intravenous injection of 1× PBS (100 μ L) for Group i) and ii), TPP (100 μ L, 2 mg/mL) for Group iii) and iv) and ExoTPP (100 μ L, 2 mg/mL) for v) and vi).

After 12 h, only the tumors of Groups ii), iv), and vi) were exposed to white light (100 mW/cm²) for 5 min. The tumor sizes were then measured every other day to calculate the volumes. The tumor volume was calculated by measuring the width and length of the tumor. Specifically, the product of the square of the width with the length was calculated, and one half of this value was taken as the tumor volume. At the point of termination, the tumor tissues from all mice were collected to take photos and for H&E staining.

***In vivo* biosafety assessment**

Healthy BALB/c mice (6 in total) were randomly divided into two groups (3 in each group) and intravenously injected with 1× PBS (100 μ L) and ExoTPP (100 μ L, 2 mg/mL), respectively. The blood samples were collected on day 7. The serum biochemistry data, including alanine aminotransferase (ALT), serum albumin (ALB), aspartate aminotransferase (AST), total serum cholesterol (TCH), total protein, and

urea, were measured by an automatic biochemical analyzer MS-480 (Meikangshengde Biotechnology Co., Ltd, China). In addition, hematocrit (HCT), lymphocytes (Lym), mean corpuscular hemoglobin (MCH), mean corpuscular hemoglobin concentration (MCHC), blood platelet (PLT), red blood cell (RBC), hemoglobin (HGB), and the white blood cell (WBC) were measured by an automatic animal five classification blood cell analyzer DF-52Vet (Dymind Biotechnology Co., Ltd, China). The organs were also collected for H&E staining.

Statistical analysis

Data are shown as Mean \pm standard error of the mean (s.e.m.). All data were normally distributed. Statistical analysis was performed using Prism Software (GraphPad, USA). Student's t-test was performed, and the significance was defined as P-values < 0.05 , 0.01 , or 0.001 , respectively.

Notes and references

1. Y. Li, Z. Li, D. Hu, S. Wang, M. Zha, S.-B. Lu, Z. Sheng and K. Li, *Chem. Commun.*, 2021, 57, 6420.
2. S. Li, S. Hao, Y. Yang, Y. He, C. Long, Z. Zhang and J. Zhang, *Chem. Commun.*, 2023, 59, 591.
3. G. Yang, S.-B. Lu, C. Li, F. Chen, N. Jen-Shyang, M. Zha, Y. Li, J. Gao, T. Kang, C. Liu and K. Li, *Chem. Sci.*, 2021, 12, 14773.
4. Y. Li, J.-Y. Wu, J.-M. Wang, X.-B. Hu, J.-X. Cai and D. Xiang, *Acta Biomater.*, 2020, 101, 519.

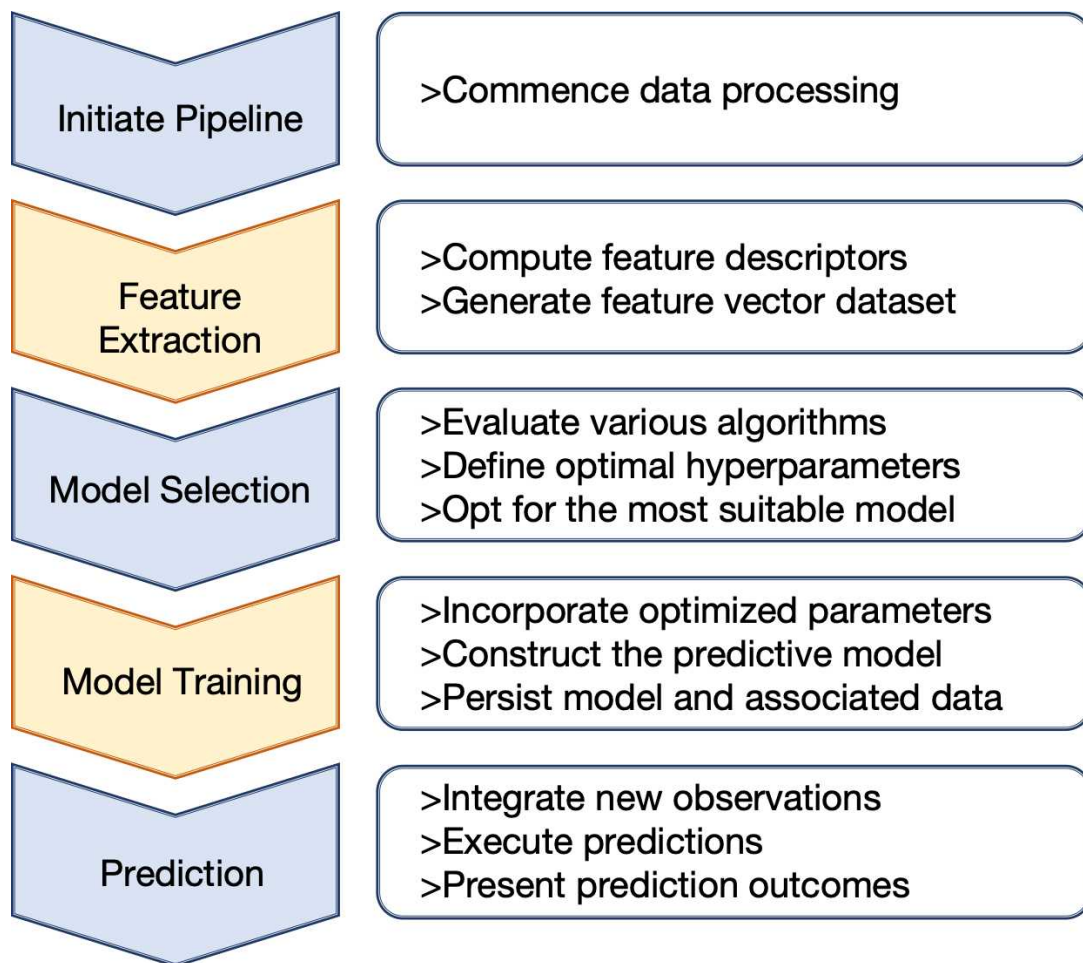


Fig. S1. The sequential stages of a machine learning pipeline.

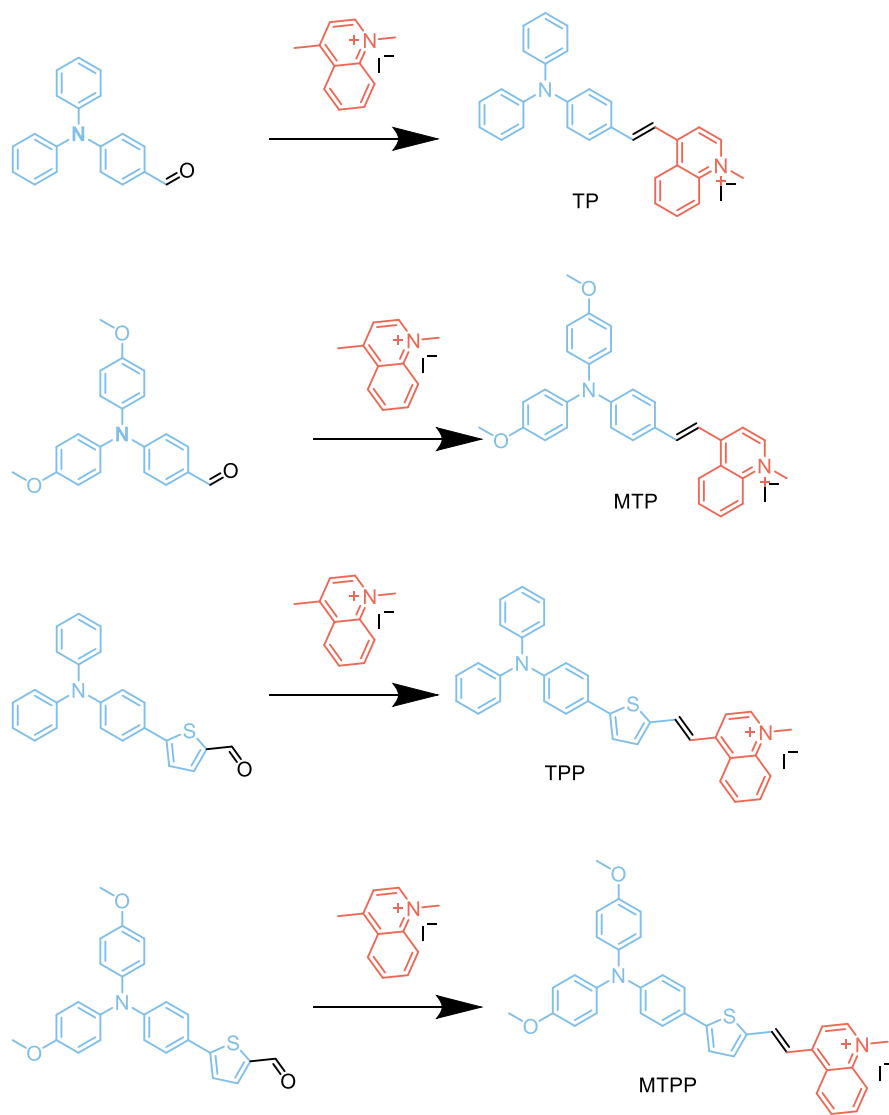


Fig. S2. Synthesis process of TP, MTP, TPP, and MTPP.

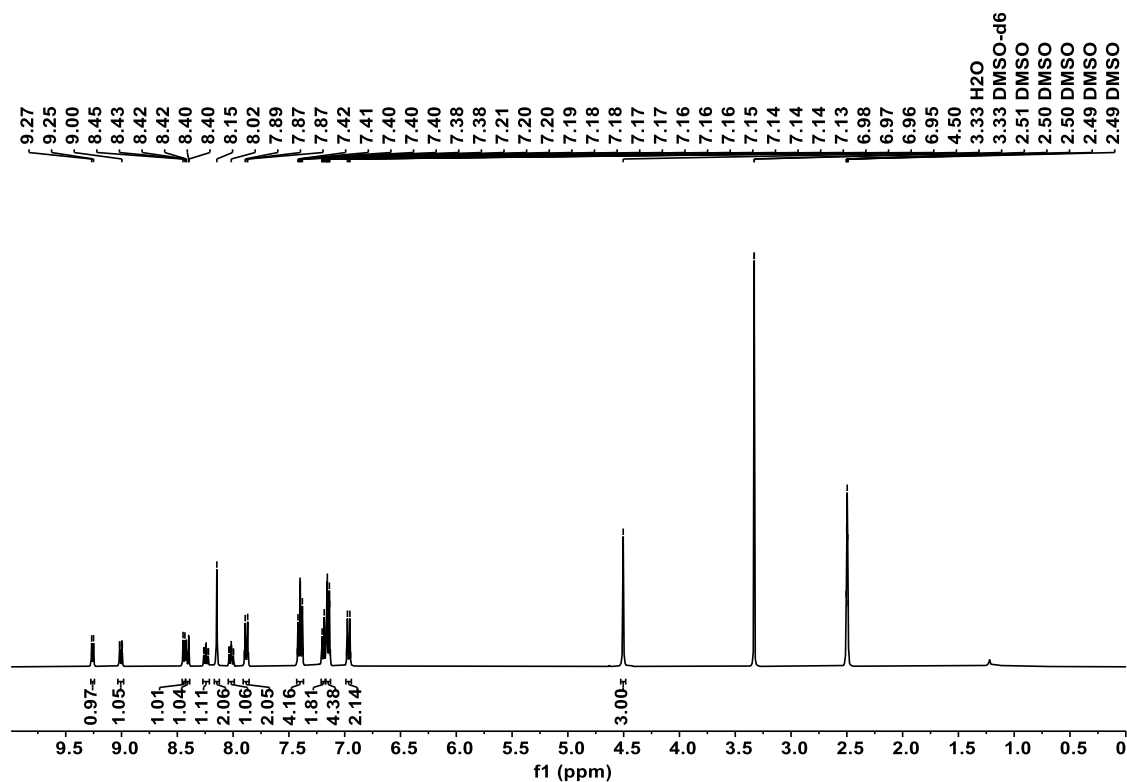


Fig. S3. The ^1H NMR spectrum of TP in DMSO-d_6 .

^1H NMR (400 MHz, DMSO-d_6 , δ ppm): 9.26 (d, $J = 6.4$ Hz, 1H), 9.01 (dd, $J = 8.8, 1.6$ Hz, 1H), 8.44 (d, $J = 6.8$ Hz, 1H), 8.41 (dd, $J = 8.89, 1.2$ Hz, 1H), 8.24 (ddd, $J = 8.8, 6.8, 1.2$ Hz, 1H), 8.15 (s, 2H), 8.02 (ddd, $J = 8.4, 7.2, 1.2$ Hz, 1H), 7.91 – 7.86 (m, 2H), 7.43 – 7.37 (m, 4H), 7.19 (dt, $J = 7.6, 1.2$ Hz, 2H), 7.17 – 7.13 (m, 4H), 6.99 – 6.94 (m, 2H), 4.50 (s, 3H)

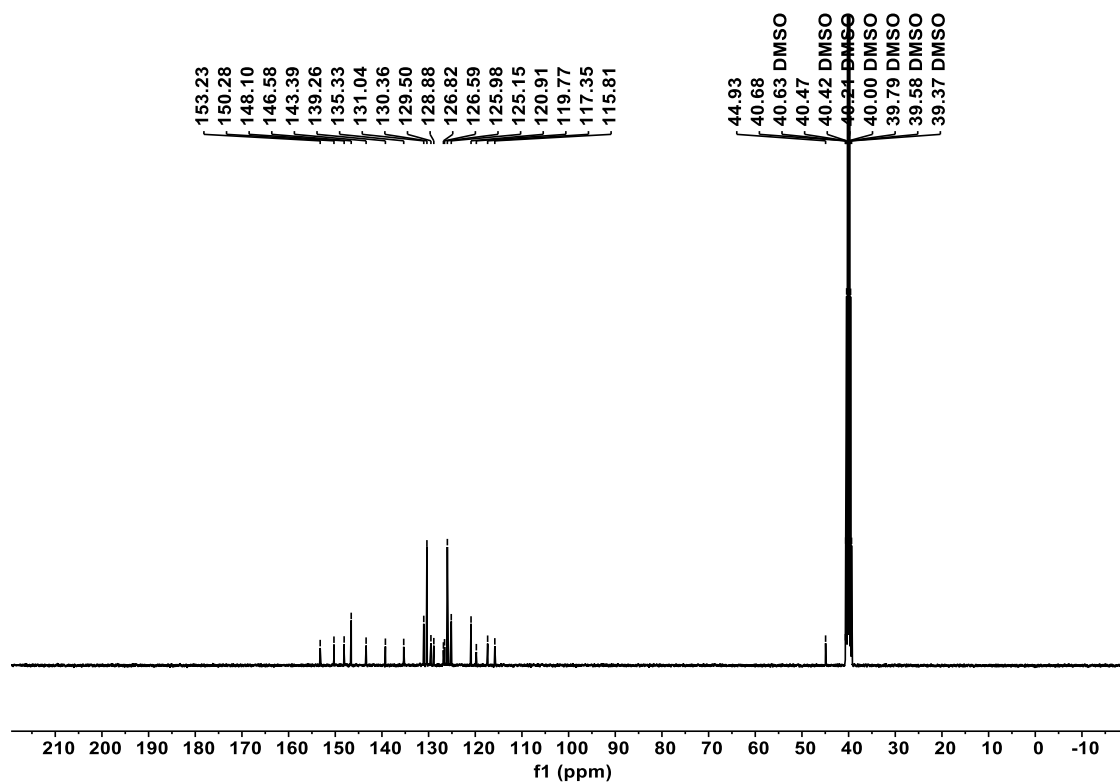


Fig. S4. The ^{13}C NMR spectrum of TP in DMSO- d_6 .

^{13}C NMR (100 MHz, DMSO- d_6 , δ ppm): 44.93, 115.81, 117.35, 119.77, 120.91, 125.15, 125.98, 126.59, 126.82, 128.88, 129.50, 130.36, 131.04, 135.33, 139.26, 143.39, 146.58, 148.10, 150.28, 153.23.

Positive mode

1 #9 RT: 0.08 AV: 1 NL: 3.00E9
T: FTMS + p ESI Full ms [100.0000-1500.0000]

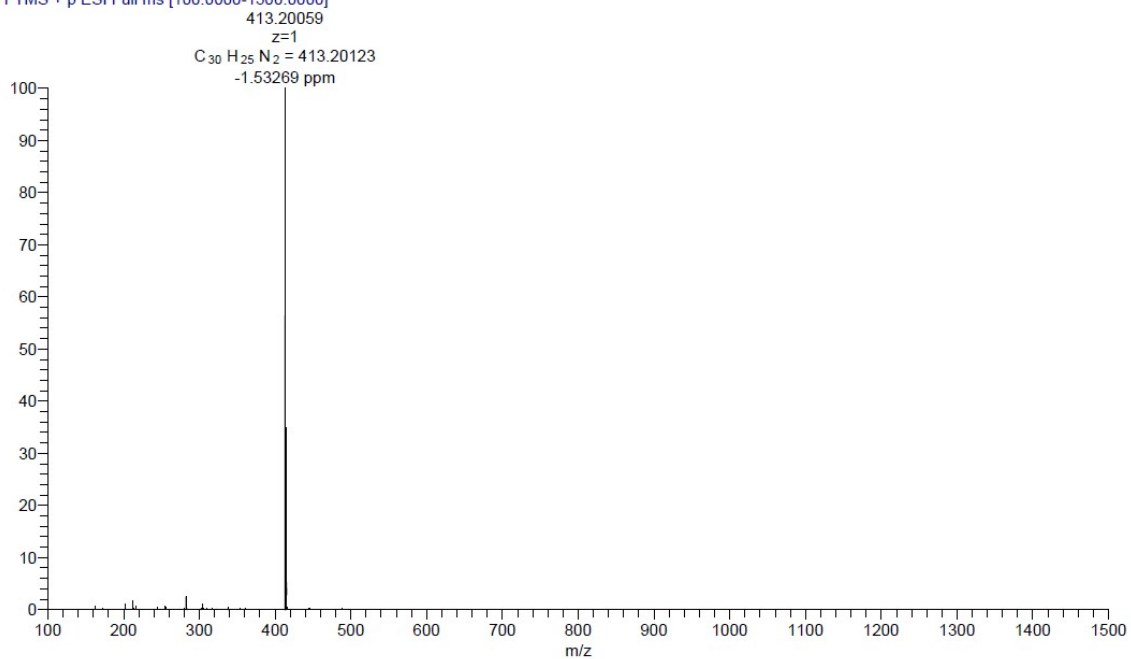


Fig. S5. The HRMS of TP.

m/z calcd. for C₃₀H₂₅N₂⁺ ([M]⁺), 413.20123; found, 413.20059.

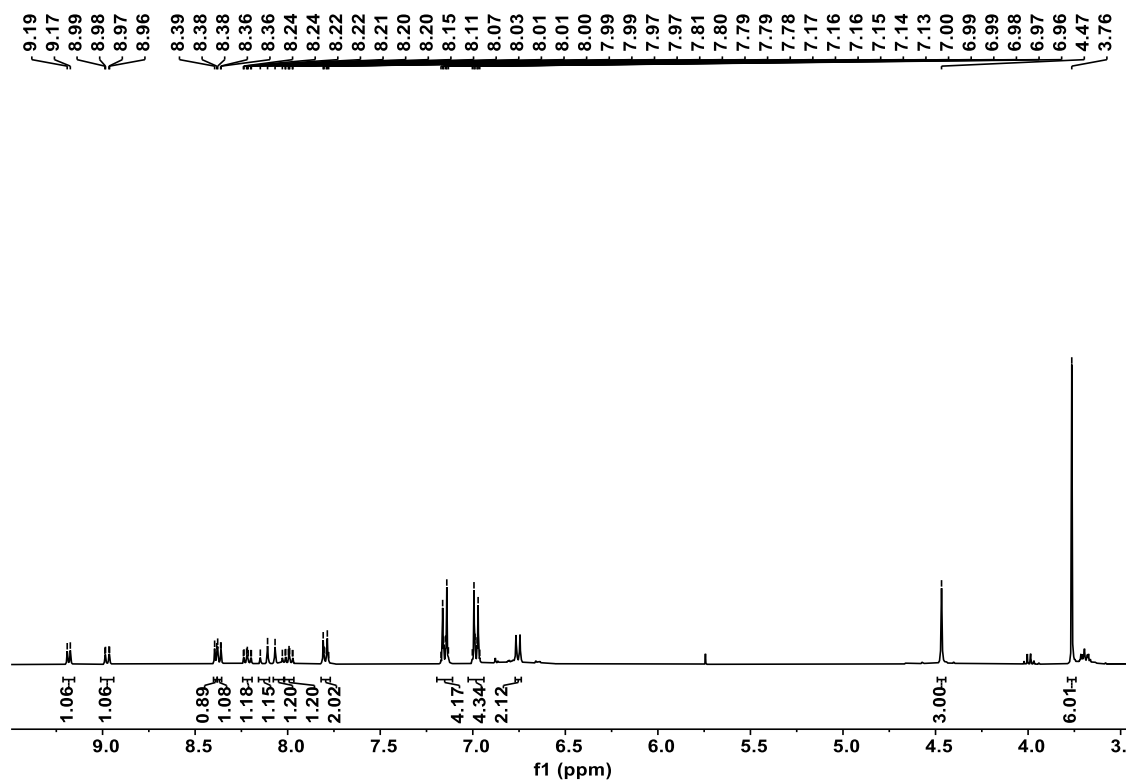


Fig. S6. The ^1H NMR spectrum of MTP in DMSO-d_6 .

^1H NMR (400 MHz, DMSO-d_6 , δ ppm) 9.18 (d, $J = 6.7$ Hz, 1H), 8.97 (dd, $J = 8.8, 1.3$ Hz, 1H), 8.39 (d, $J = 4.5$ Hz, 1H), 8.38 – 8.36 (m, 1H), 8.22 (ddd, $J = 8.7, 6.9, 1.3$ Hz, 1H), 8.13 (d, $J = 15.7$ Hz, 1H), 8.05 (d, $J = 15.8$ Hz, 1H), 7.99 (ddd, $J = 8.3, 6.9, 1.1$ Hz, 1H), 7.82 – 7.77 (m, 2H), 7.19 – 7.11 (m, 4H), 7.02 – 6.94 (m, 4H), 6.77 – 6.74 (m, 2H), 4.47 (s, 3H), 3.76 (s, 6H).

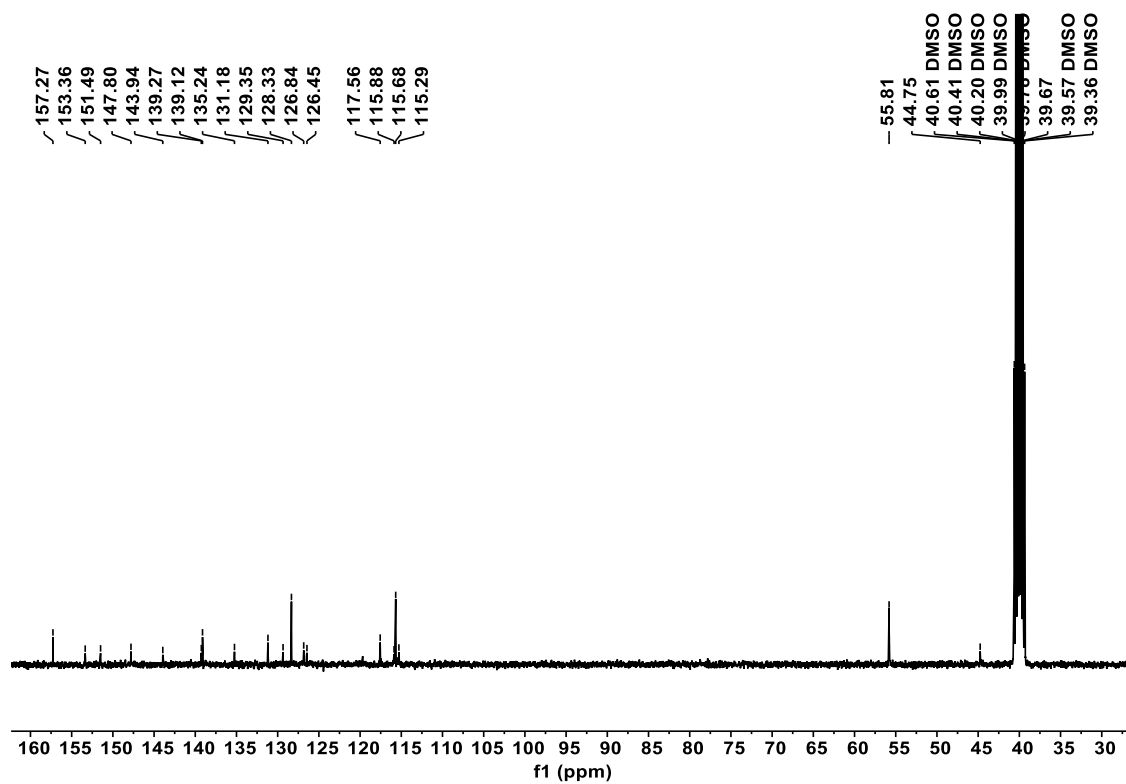


Fig. S7. The ^{13}C NMR spectrum of MTP in DMSO-d_6 .

^{13}C NMR (100 MHz, DMSO-d_6 , δ ppm): 44.75, 55.81, 115.29, 115.68, 115.88, 117.56, 126.45, 126.84, 128.33, 129.35, 131.18, 135.24, 139.12, 139.27, 143.94, 147.80, 151.49, 153.36, 157.27.

Positive mode

2 #11 RT: 0.10 AV: 1 NL: 2.92E9
T: FTMS + p ESI Full ms [100.0000-1500.0000]

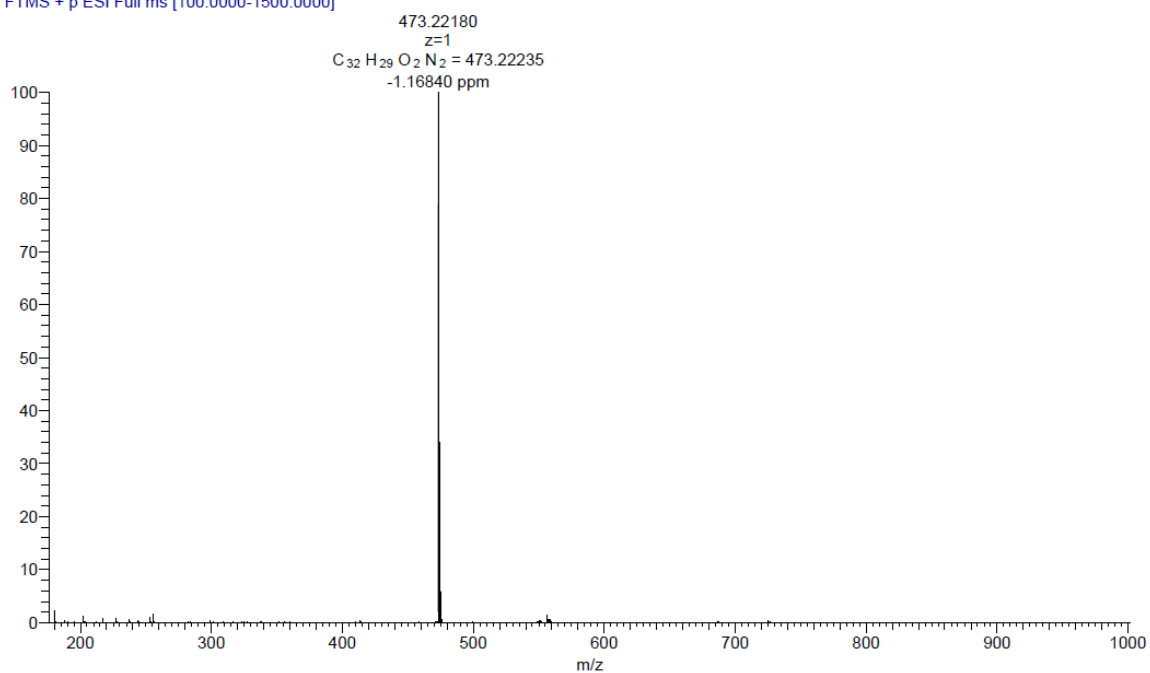


Fig. S8. The HRMS of MTP.

m/z calcd. for C₃₂H₂₉N₂O₂⁺ ([M]⁺), 473.22235; found, 473.22180.

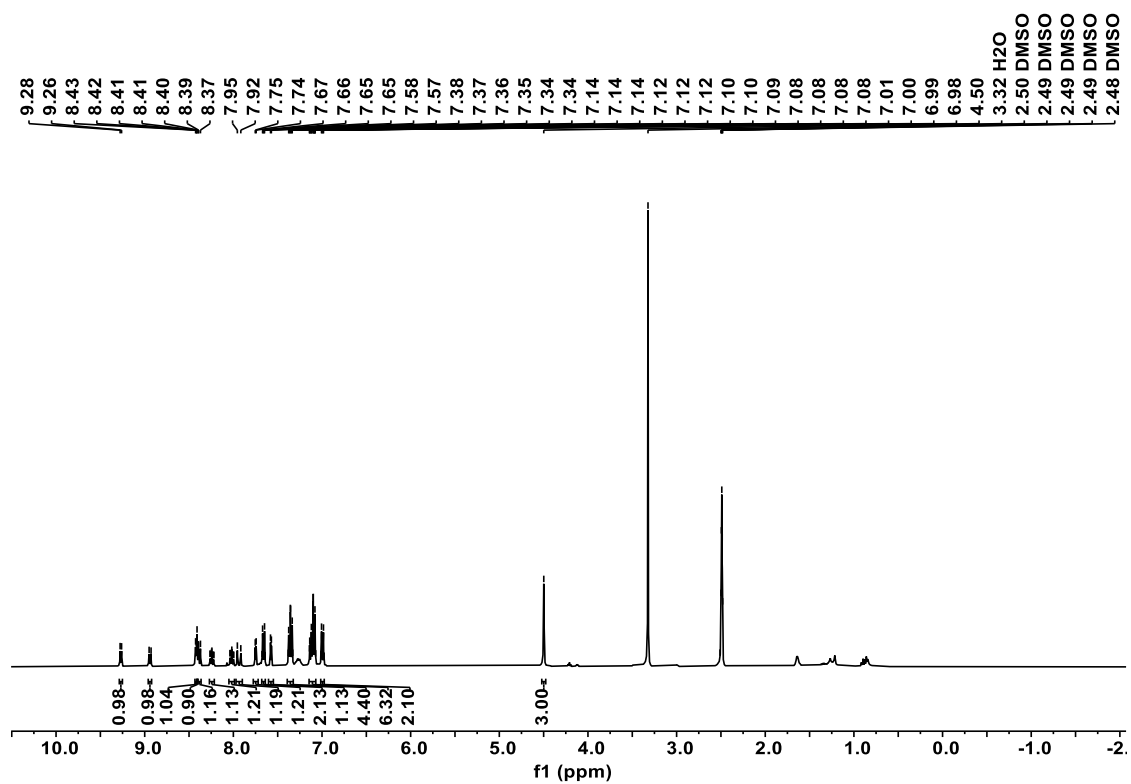


Fig. S9. The ^1H NMR spectrum of TPP in $\text{DMSO-}d_6$.

^1H NMR (400 MHz, $\text{DMSO-}d_6$, δ ppm): 9.30 (s, 1H), 8.95 (s, 1H), 8.42 (s, 2H), 8.26 (s, 1H), 8.15– 7.85 (m, 2H), 7.67 (t, $J = 36$ Hz, 4H), 7.48 – 6.70 (m, 12H), 4.51 (s, 3H).

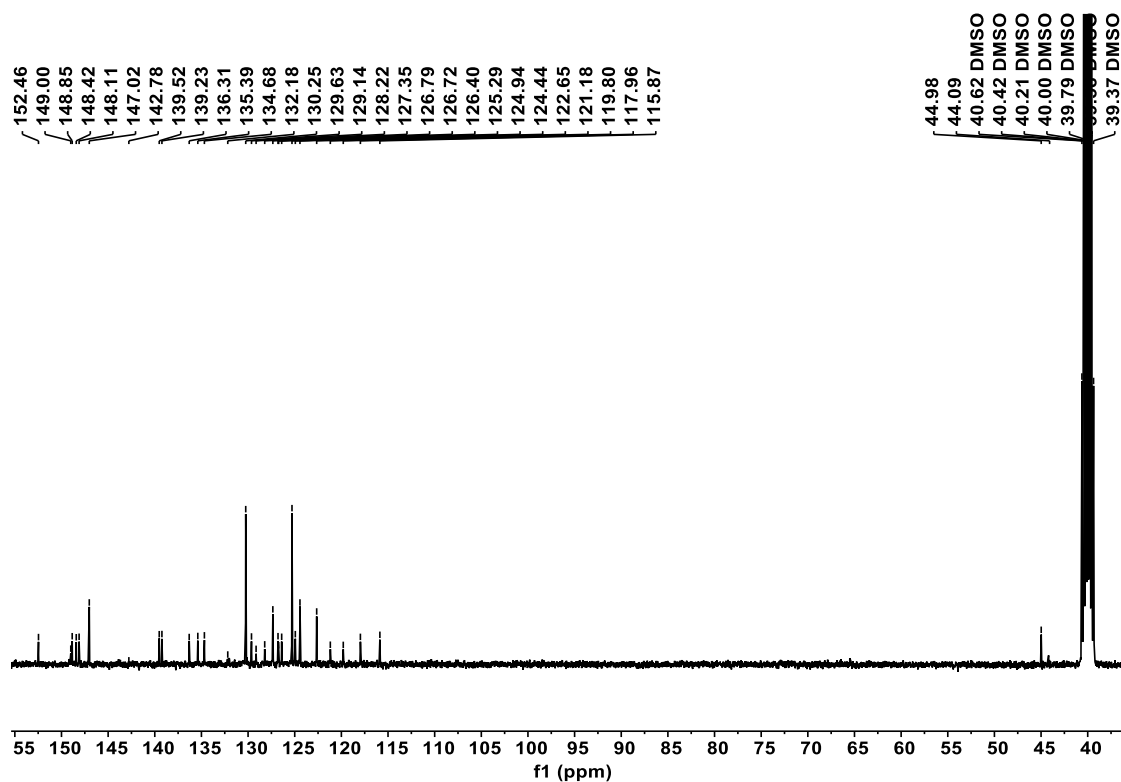


Fig. S10. The ^{13}C NMR spectrum of TPP in $\text{DMSO-}d_6$.

^{13}C NMR (100 MHz, $\text{DMSO-}d_6$, δ ppm): 44.99, 115.85, 117.90, 119.78, 122.14, 122.63, 124.43, 124.58, 124.92, 125.28, 125.45, 125.96, 126.36, 126.70, 126.77, 127.33, 127.89, 129.62, 130.25, 134.70, 135.37, 136.30, 139.21, 139.52, 140.00, 141.31, 146.87, 147.01, 148.08, 148.39, 148.84, 152.42, 153.38, 184.19.

Positive mode

3 #9 RT: 0.08 AV: 1 NL: 2.60E9

T: FTMS + p ESI Full ms [100.0000-1500.0000]

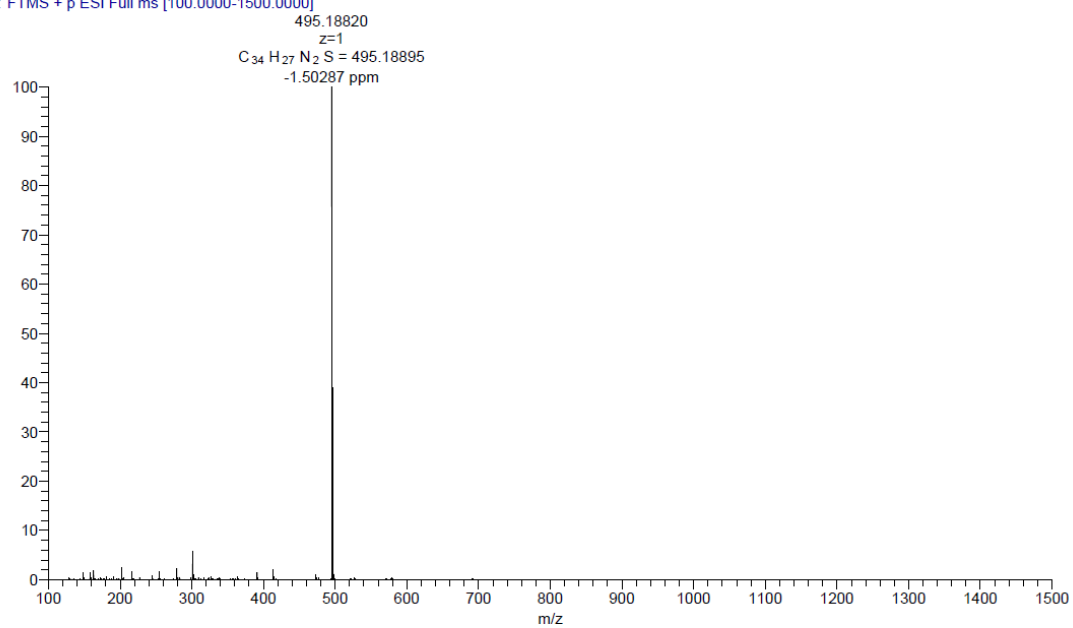


Fig. S11. The HRMS of TPP.

m/z calcd. for C₃₄H₂₇N₂S⁺ ([M]⁺), 495.18895; found, 495.18820.

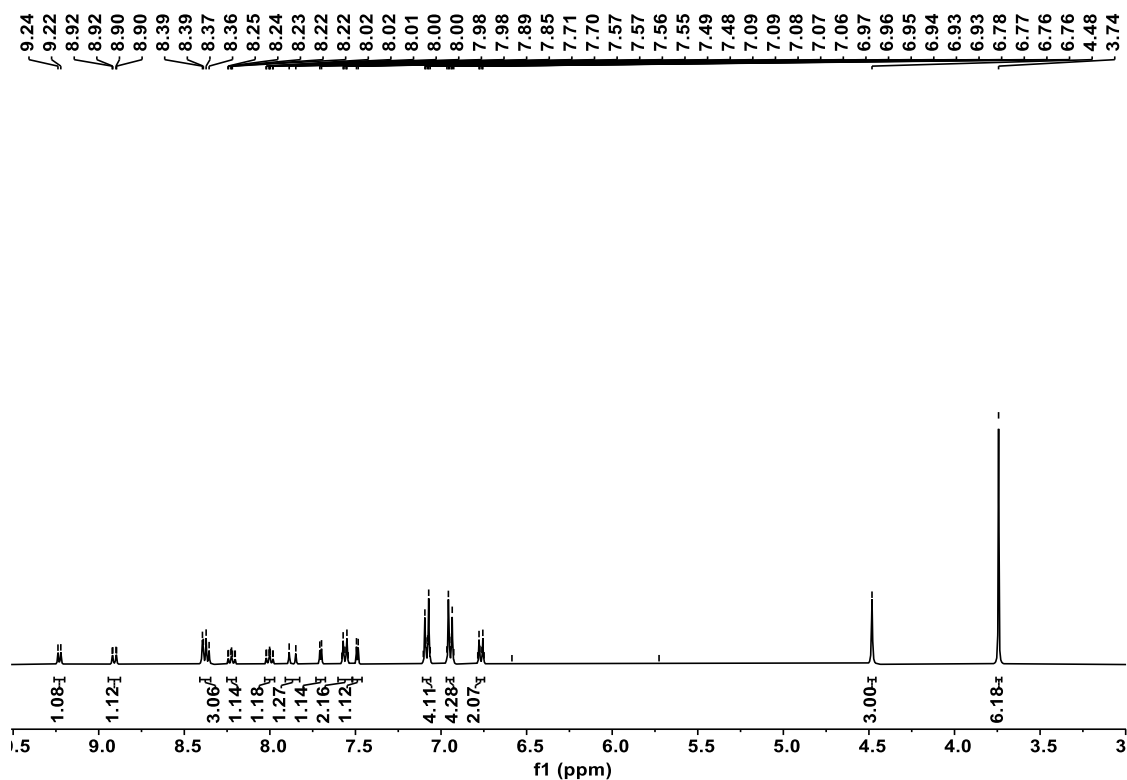


Fig. S12. The ^1H NMR spectrum of MTPP in $\text{DMSO}-d_6$.

^1H NMR (400 MHz, $\text{DMSO}-d_6$, δ ppm) 9.23 (d, $J = 6.7$ Hz, 1H), 8.91 (dd, $J = 8.8, 1.4$ Hz, 1H), 8.41 – 8.35 (m, 3H), 8.22 (ddd, $J = 8.6, 6.9, 1.3$ Hz, 1H), 8.00 (ddd, $J = 8.3, 6.9, 1.0$ Hz, 1H), 7.87 (d, $J = 15.5$ Hz, 1H), 7.70 (d, $J = 4.0$ Hz, 1H), 7.60 – 7.52 (m, 2H), 7.49 (d, $J = 4.0$ Hz, 1H), 7.11 – 7.06 (m, 4H), 6.97 – 6.93 (m, 4H), 6.79 – 6.75 (m, 2H), 4.48 (s, 3H).

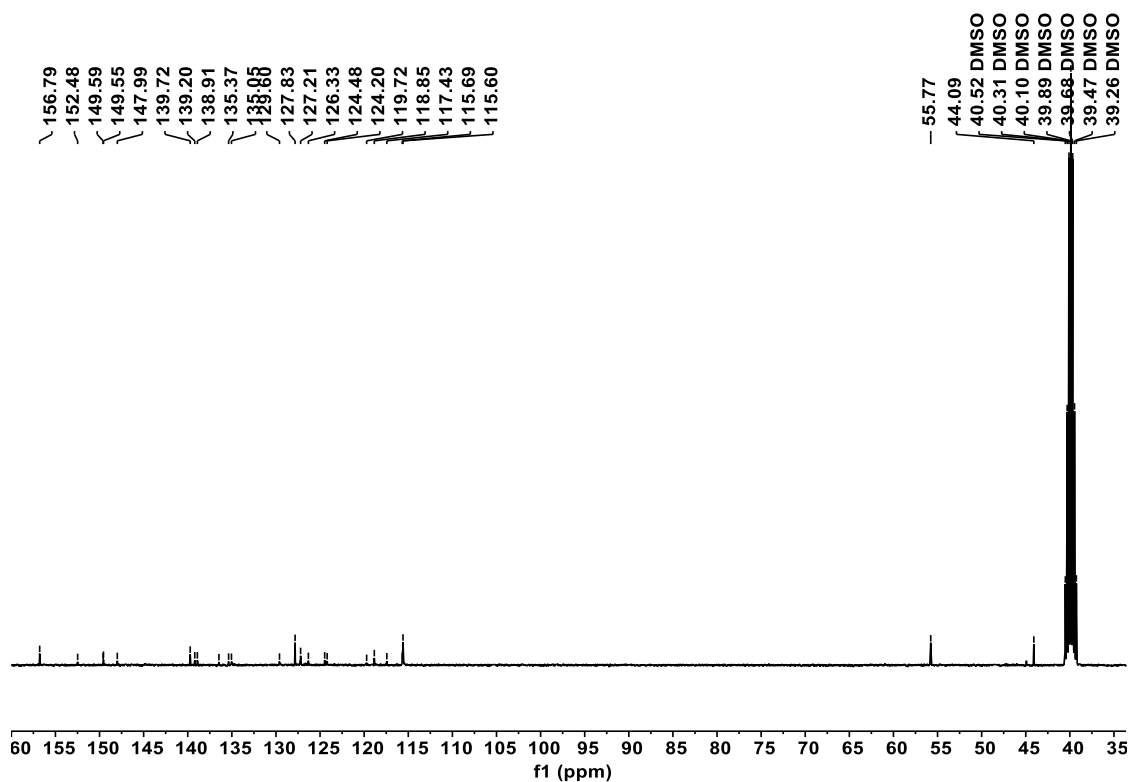


Fig. S13. The ^{13}C NMR spectrum of MTPP in $\text{DMSO-}d_6$.

^{13}C NMR (100 MHz, $\text{DMSO-}d_6$, δ ppm): 44.09, 55.77, 115.60, 115.69, 117.43, 118.85, 119.72, 124.20, 124.48, 126.33, 127.21, 127.83, 129.60, 135.05, 135.37, 138.91, 139.20, 139.72, 147.99, 149.55, 149.55, 149.59, 152.48, 156.79

Positive mode

4 #7 RT: 0.06 AV: 1 NL: 8.42E8

T: FTMS + p ESI Full ms [100.0000-1500.0000]

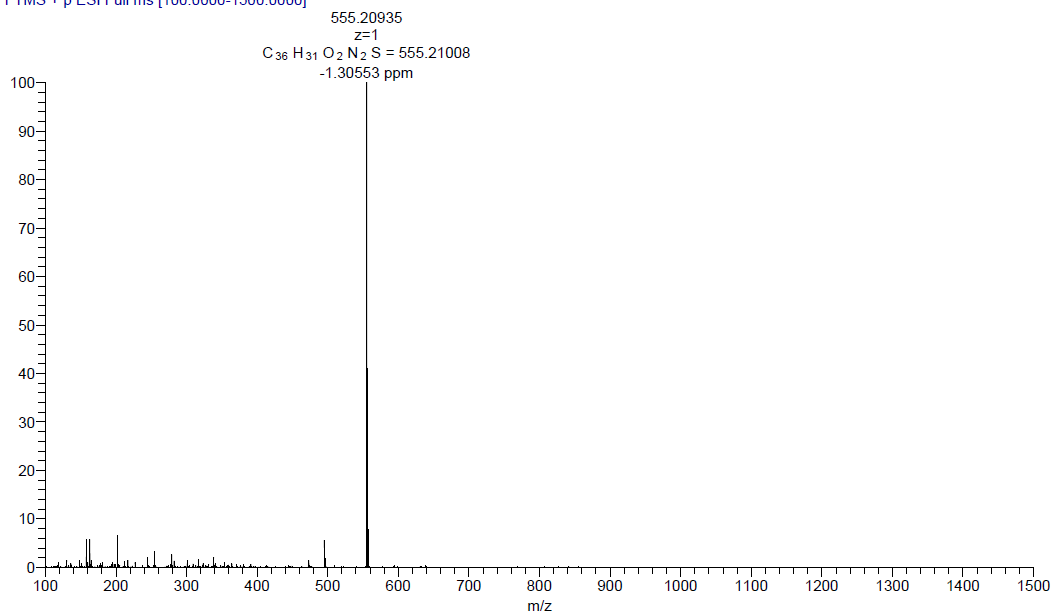


Fig. S14. The HRMS of MTPP.

m/z calcd. for C₃₆H₃₁N₂O₂S⁺ ([M]⁺), 555.21008; found, 555.20935.

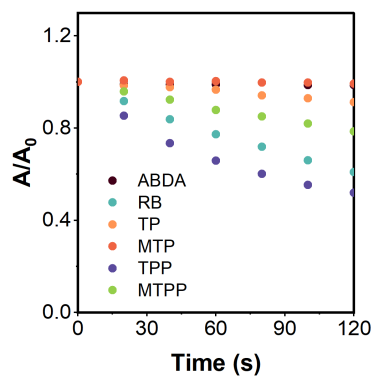


Fig. S15. The singlet oxygen production of ABDA, RB, TP, MTP, TPP, and MTPP (10 μM).

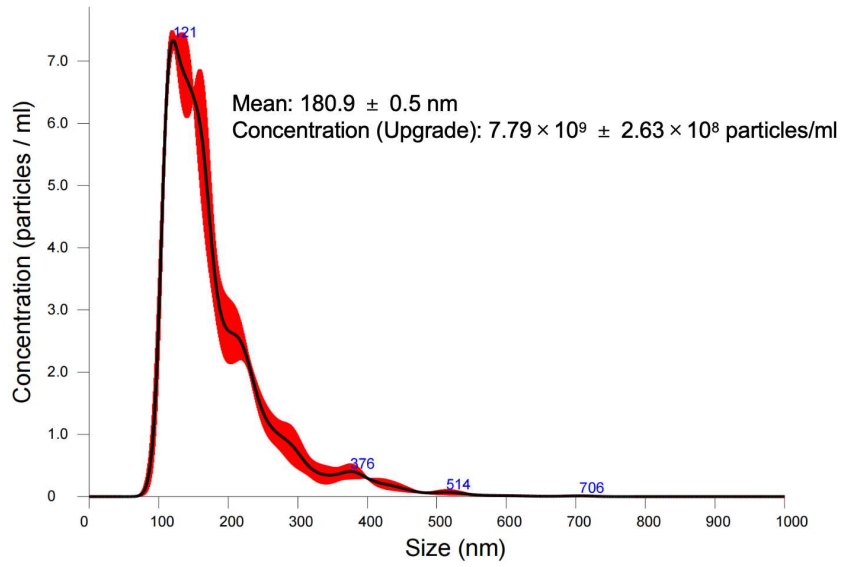


Fig. S16. NTA analysis of 4T1 exosomes.

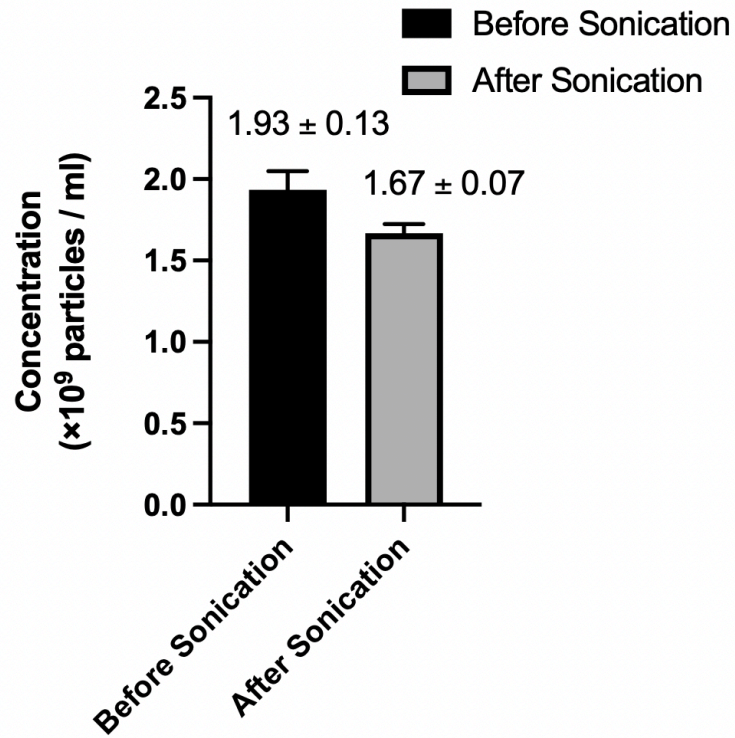


Fig. S17. The concentration of exosomes before and after sonication, measured by NTA.

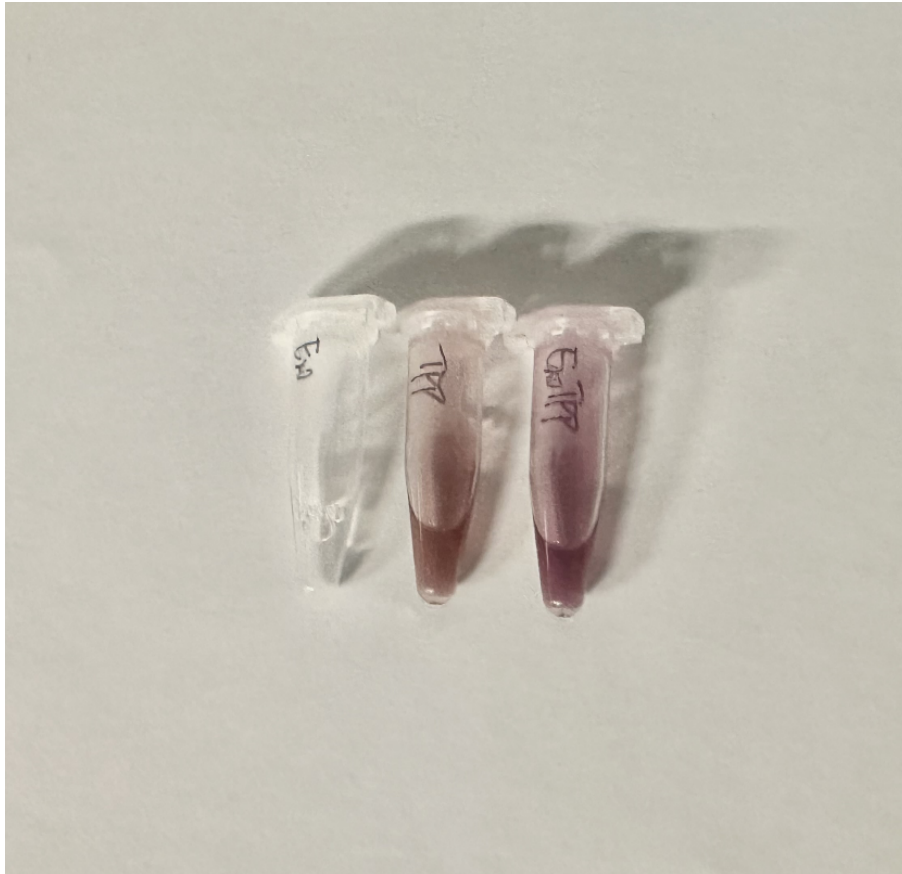


Fig. S18. Photograph of Exosomes, TPP, and ExoTPP.

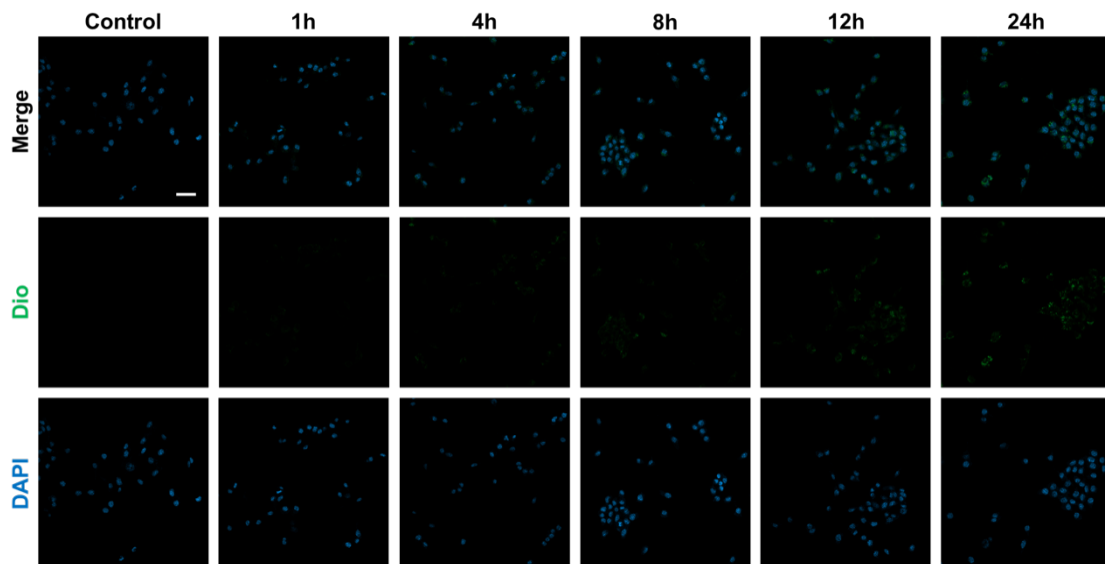


Fig. S19. Autologous 4T1 cellular uptake of 4T1 exosomes. 4T1 cells were incubated with Dio-labeled 4T1 exosomes for 1, 4, 8, 12 and 24 h before imaging. Scale bar: 50 μm .

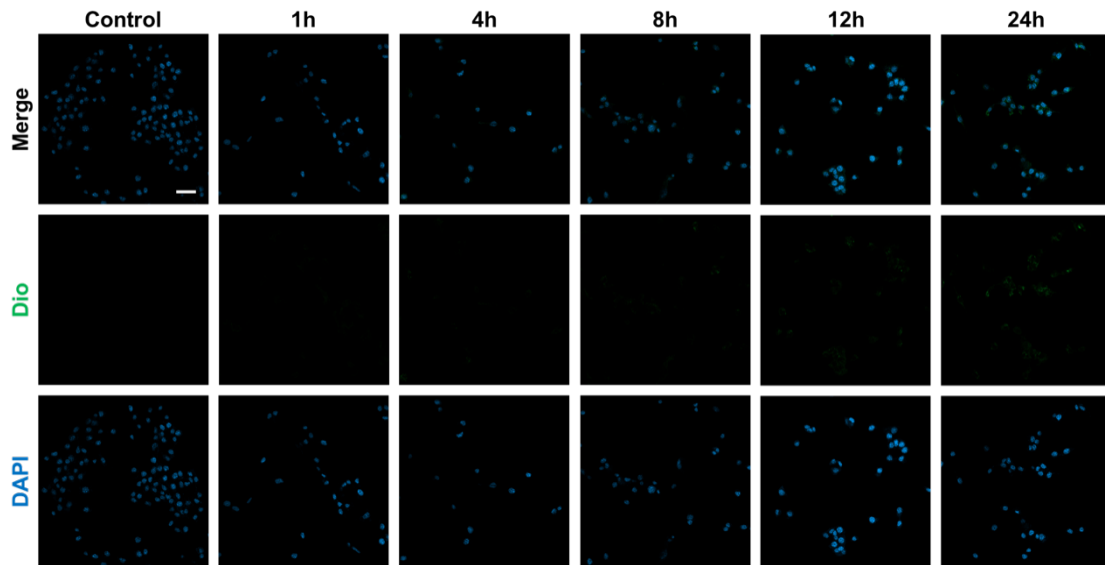


Fig. S20. Heterologous 4T1 cellular uptake of HeLa exosomes. 4T1 cells were incubated with Dio-labeled HeLa exosomes for 1, 4, 8, 12, and 24 h before imaging. Scale bar: 50 μ m.

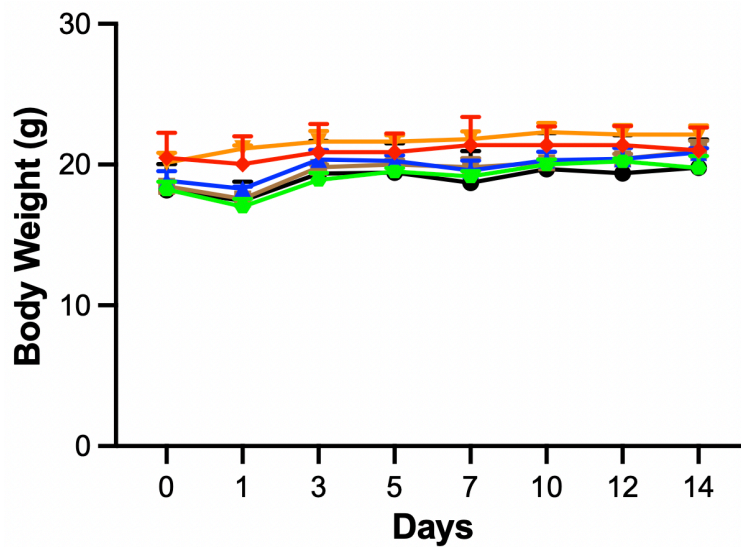


Fig. S21. Body weights of the 4T1 breast-bearing mice in the six groups.

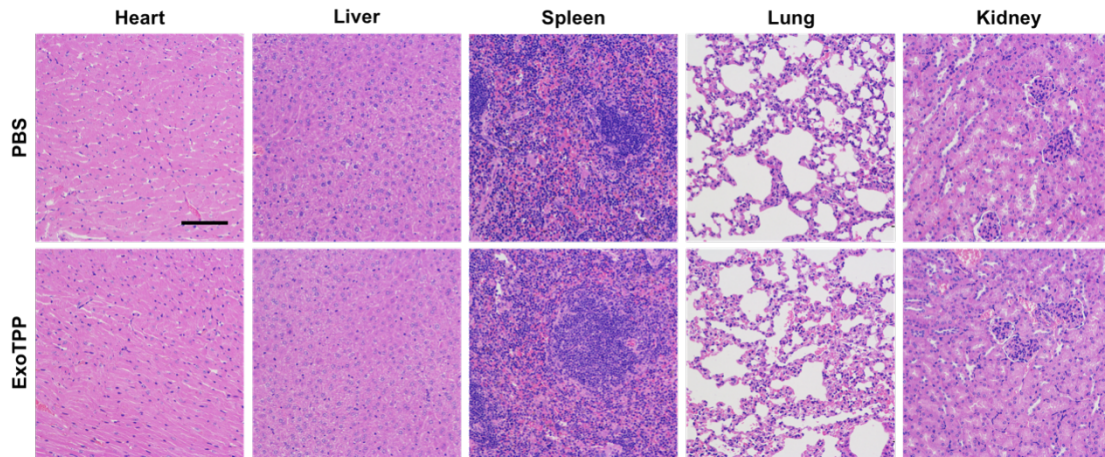


Fig. S22. Hematoxylin and eosin (H&E) staining of the sectioned tissues (heart, liver, spleen, lung, and kidney) from the BALB/c female mice injected with PBS or ExoTPP. The samples were collected on day 7 post-injection. Scale bar: 100 μ m.

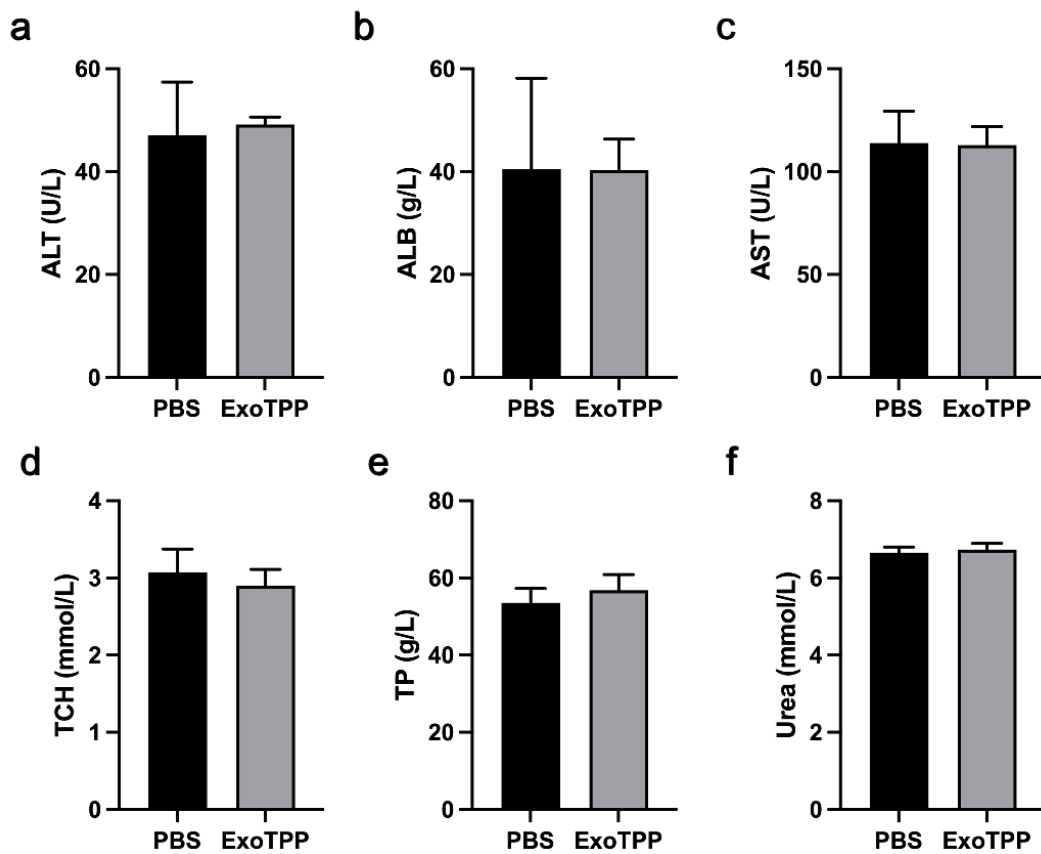


Fig. S23. Serum biochemistry data. The levels of (a) alanine aminotransferase (ALT), (b) serum albumin (ALB), (c) aspartate aminotransferase (AST), (d) total serum cholesterol (TCH), (e) total protein and (f) Urea in samples collected from the control and ExoTPP treated mice (n = 3).

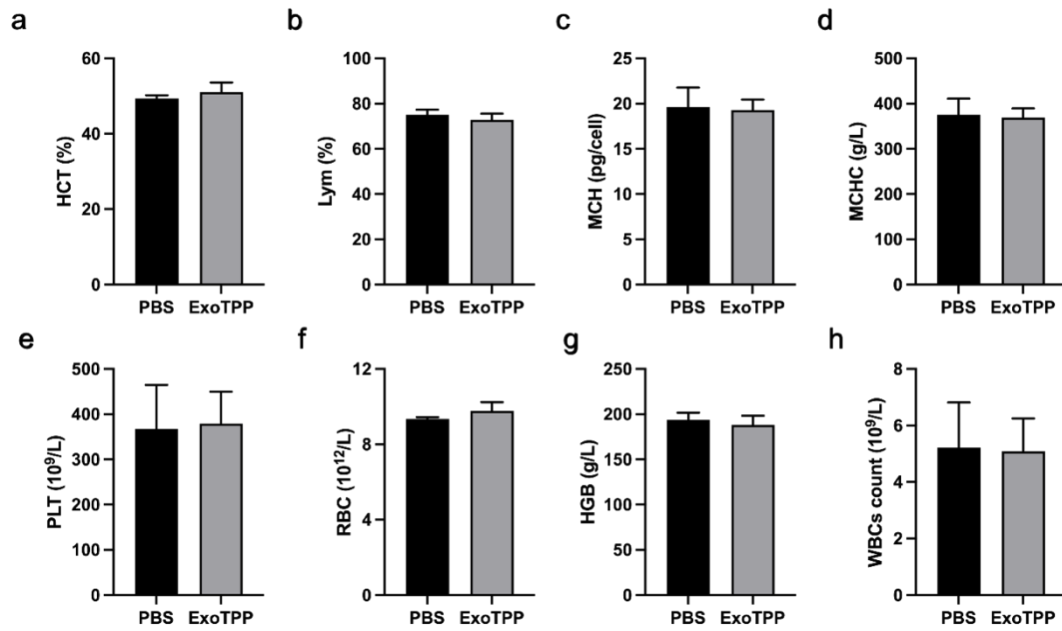


Fig. S24. Blood routine analysis. The numbers of (a) hematocrit (HCT), (b) lymphocytes (Lym), (c) mean corpuscular hemoglobin (MCH), (d) mean corpuscular hemoglobin concentration (MCHC), (e) blood platelet (PLT), (f) red blood cell (RBC), (g) hemoglobin (HGB) and (h) white blood cell (WBC) in samples collected from the control and ExoTPP treated mice (n = 3).

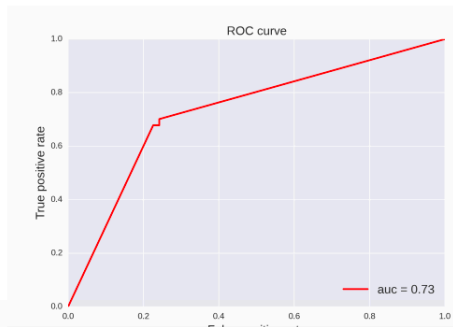
Report for DT:

> Model selection

Selected method and the parameters

> Model building

The trained model and the model performance

1	Accuracy	0.725
2	F1 score	0.67
3	Cross-validation fold	10
4	MCC	0.435
5	Number of negative samples	124
6	Number of positive samples	87
7	AUC score	0.732
8	Sensitivity	0.678
9	Specificity	0.758
10	parameter	{}
11	ROC curve	 <p>The figure is a Receiver Operating Characteristic (ROC) curve plot. The x-axis is labeled 'False positive rate' and ranges from 0.0 to 1.0. The y-axis is labeled 'True positive rate' and ranges from 0.0 to 1.0. A red line represents the ROC curve, starting at (0,0) and ending at (1,1). The curve rises steeply from the origin to approximately (0.2, 0.7), then continues to rise more gradually towards (1,1). A legend in the bottom right corner indicates 'auc = 0.73'. The plot is titled 'ROC curve'.</p>

Report for GNB:

> Model selection

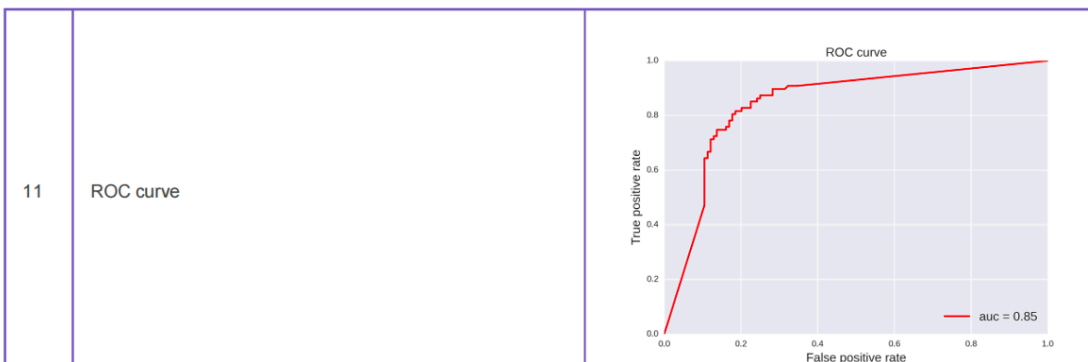
Selected method and the parameters

1	Cross-validation fold	10
2	Number of negative samples	124
3	Best parameters	{'nb_type': 'GaussianNB'}
4	Number of positive samples	87
5	The mean score for each iteration	0.764502164502
6	Parameters	{'nb_type': 'GaussianNB'}

> Model building

The trained model and the model performance

1	Accuracy	0.81
2	F1 score	0.775
3	Cross-validation fold	10
4	MCC	0.612
5	Number of negative samples	124
6	Number of positive samples	87
7	AUC score	0.847
8	Sensitivity	0.793
9	Specificity	0.823
10	parameter	{'nb_type': 'GaussianNB'}



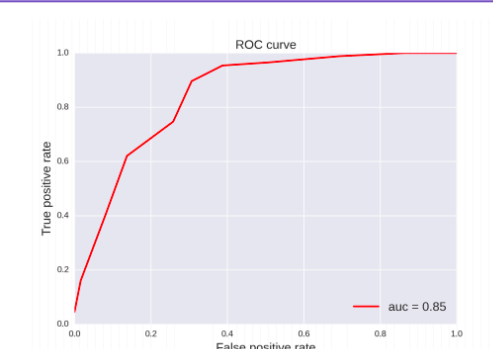
Report for KNN:

> Model selection

Selected method and the parameters

> Model building

The trained model and the model performance

1	Accuracy	0.744
2	F1 score	0.707
3	Cross-validation fold	10
4	MCC	0.483
5	Number of negative samples	124
6	Number of positive samples	87
7	AUC score	0.849
8	Sensitivity	0.747
9	Specificity	0.742
10	parameter	{'n_neighbors': '10'}
11	ROC curve	 <p>The figure is a Receiver Operating Characteristic (ROC) curve plot. The x-axis is labeled 'False positive rate' and ranges from 0.0 to 1.0. The y-axis is labeled 'True positive rate' and also ranges from 0.0 to 1.0. A red curve starts at (0,0) and rises steeply, crossing the diagonal line at approximately (0.1, 0.6). It continues to rise, reaching a true positive rate of about 0.95 at a false positive rate of 0.4, and then levels off towards (1,1). A legend in the bottom right corner indicates 'auc = 0.85'.</p>

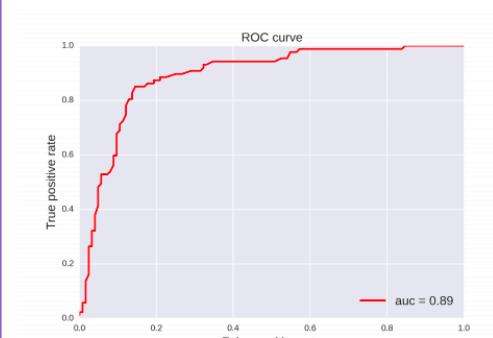
Report for RFM:

> Model selection

Selected method and the parameters

> Model building

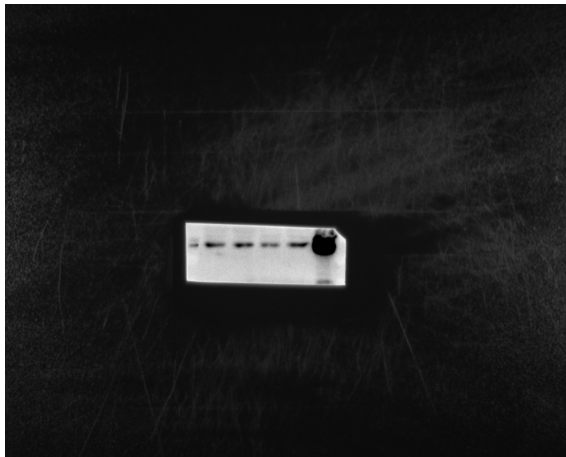
The trained model and the model performance

1	Accuracy	0.839
2	F1 score	0.805
3	Cross-validation fold	10
4	MCC	0.668
5	Number of negative samples	124
6	Number of positive samples	87
7	AUC score	0.891
8	Sensitivity	0.805
9	Specificity	0.863
10	parameter	{'n_estimators': 100, 'max_features': 5, 'oob_score': False}
11	ROC curve	 <p>The figure is a Receiver Operating Characteristic (ROC) curve plot. The x-axis is labeled 'False positive rate' and ranges from 0.0 to 1.0. The y-axis is labeled 'True positive rate' and also ranges from 0.0 to 1.0. A red curve starts at (0,0) and rises steeply, reaching a true positive rate of approximately 0.8 at a false positive rate of 0.1. The curve then continues to rise more gradually, reaching a true positive rate of 1.0 at a false positive rate of approximately 0.6. A legend in the bottom right corner indicates 'auc = 0.89'.</p>

Full raw data for the western blot experiments: (The rightmost column is the group of Cell Lysates)



CD9



TSG101



Calnexin